Raman Spectroscopic Measurement of Oxidation in Supercritical Water. 2. Conversion of Isopropyl Alcohol to Acetone

Thomas B. Hunter, Steven F. Rice*, and Russell G. Hanush

Combustion Research Facility, Sandia National Laboratories, P.O. Box 969, Livermore, California 94551-0969

Ind. Eng. Chem. Res., **1996**, *35* (11), pp 3984–3990

DOI: 10.1021/ie9505118

Publication Date (Web): November 7, 1996

Abstract

The oxidation of isopropyl alcohol in supercritical water has been investigated using Raman spectroscopy. Results for species concentration as a function of residence-time are presented for temperatures ranging from 400 to 480 °C at constant pressure, 24.4 ± 0.3 MPa, and constant equivalence ratio, 0.88 ± 0.02. Acetone has been identified as the principal intermediate formed and subsequently destroyed, during the oxidation process. By assuming first-order kinetics for the destruction of both isopropyl alcohol and acetone, effective first-order rate constants have been determined from fits of the experimental data. Assuming Arrhenius behavior, the fits yield rate constants for isopropyl alcohol, $k_{eff,ipa} = 3.255 \times 10^{22}(s^{-1}) \exp[-301.1(kJ \cdot mol^{-1})/RT]$, and for acetone, $k_{eff,ace} = 1.948 \times 10^{10}(s^{-1}) \exp[-137.7(kJ \cdot mol^{-1})/RT]$. These results indicate that for temperatures greater than 425 °C, the destruction of isopropyl alcohol proceeds faster than that of acetone.

Raman Spectroscopic Measurement of Oxidation in Supercritical Water. II. Conversion of Isopropanol to Acetone

Thomas B. Hunter, Steven F. Rice*, and Russell G. Hanush

Combustion Research Facility, Sandia National Laboratories, Livermore, CA 94551-0969
*(*Corresponding Author)*

manuscript submitted to: Industrial and Engineering Chemistry Research

ABSTRACT

The oxidation of isopropanol in supercritical water has been investigated using Raman spectroscopy. Results for species concentration as a function of residence–time results are presented for temperatures ranging from 400 to 480 °C at constant pressure, 24.4 ± 0.3 MPa, and constant equivalence ratio, 0.88 ± 0.02. Acetone has been identified as the principal intermediate formed, and subsequently destroyed, during the oxidation process. By assuming first–order kinetics for the destruction of both isopropanol and acetone, effective first–order rate constants have been determined from fits of the experimental data. Assuming Arrhenius behavior, the fits yield rate constants for isopropanol, $k_{eff,ipa} = 3.255 \times 10^{22}(s^{-1})\exp\left[-301.1(kJ \cdot mol^{-1})/RT\right]$ and for acetone, $k_{eff,ace} = 1.948 \times 10^{10}(s^{-1})\exp\left[-137.7(kJ \cdot mol^{-1})/RT\right]$. These results indicate that for temperatures greater than 425 °C, the destruction of isopropanol proceeds faster than that of acetone.

BACKGROUND AND INTRODUCTION

Supercritical water oxidation (SCWO) is a promising technology for the destruction of hazardous organic waste streams, especially those containing a large aqueous fraction. A number of research groups have engaged in projects to characterize the process in order to develop commercially viable systems for the destruction of a variety of waste streams. Three excellent reviews of the SCWO process and of past research can be found in the literature (Modell, 1989;

Shaw, *et al.*, 1991; Tester, *et al.*, 1991). While much of this research has been conducted using small scale facilities, the technology is not limited to bench top experiments and research. For example, a number of private companies and national laboratories are currently involved with pilot facilities (Ahluwalia, *et al.*, 1995; Barner, *et al.*, 1992; Kemna and Kuharich, 1995; Swallow, *et al.*, 1989). In addition, a commercial facility for the treatment of long chain organics and amines was recently opened in Austin, Texas (Gloyna, *et al.*, 1994; McBrayer, 1995).

The SCWO process has a number of advantages over other waste destruction techniques. Most of these are a direct result of the unique properties of supercritical water. As the temperature and pressure of the waste stream approach and exceed the critical properties of water (T_c = 374 °C and P_c = 22.1 MPa), both the density and dielectric constant of water decrease dramatically (Modell, 1989). As a result, many organics (and gases such as O_2, CO_2, CO, and N_2) become completely miscible in water forming a single phase; thus, eliminating interphase transport limitations for the reactants. This taken in conjunction with the pressure and temperature of SCWO, which encourage increased rates of oxidation, result in a process which is capable of rapidly destroying most organic species. As a result, high destruction efficiencies (> 99.99%) can be realized for many waste streams in less than 30 seconds under typical reactor operating conditions, i.e., temperatures ranging from 500 to 650 °C and pressures of ~25 MPa (Steeper and Rice, 1993). In a review article, Tester *et. al* (1991) list 78 organics (e.g., nitrobenzene, DDT, and ethylene glycol) and 24 complex wastes (e.g., diesel fuel, polychlorinated biphenyl, and sewage sludge) which have been successfully treated using the MODAR SCWO process (Modell, 1985; Modell, 1989; Swallow, *et al.*, 1989; Thomason, *et al.*, 1990; Thomason and Modell, 1984). Because of the relatively moderate temperatures encountered in SCWO, compared, for example, to the conditions required for incineration, virtually no oxides of nitrogen or sulfur dioxide are formed (Shaw, *et al.*, 1991; Swallow, *et al.*, 1989; Tester, *et al.*, 1991). Another advantage of SCWO results from the high densities employed—approximately 300 times greater than steam at the same temperature and ambient pressure. Because of the increased density, the process equipment is more compact for a given mass flow and effluent streams are containable,

allowing them to be analyzed prior to environmental discharge. Lastly, by properly balancing the organic content and heat release of the feed, it is possible to use the heat generated in the oxidation reaction to preheat the feed stream, allowing self sustaining operation of the system and minimizing power requirements (Swallow, *et al.*, 1989). Other interesting aspects of the affects of supercritical fluids on reaction chemistry are discussed in a review by Brennecke (1991).

While the SCWO process has a number of advantages, it does have, as all waste destruction techniques do, some engineering difficulties and drawbacks. Three of the most challenging engineering dilemmas preventing widespread commercialization of the process are: corrosion of reactor materials; scaling and plugging of the reactor; and reactor scale–up (Barner, *et al.*, 1992). The motivation for the work in this paper revolves around issues relating to scale–up of the SCWO process from bench top experiments to commercial reactor systems.

A key issue in designing efficient reactor systems is understanding the chemistry occurring in the oxidation of the waste stream. If a model could be developed that predicts the time–resolved results of the oxidation process, reactor systems could be designed to exacting specifications. Ultimately, this would allow the destruction of target species in the most time– and energy–efficient, which translates into cost–efficient, manner. Such a model would also allow designers to predict the concentrations that would be present in each of the effluent streams for a given waste feed, again allowing designs to be tailored to produce acceptable effluent levels of various controlled species. Finally, the model would allow calculation of heat release profiles within the reactor system for design safety considerations. To accomplish these tasks, the model must effectively reproduce the detailed SCWO process chemistry, including the intermediate species formed and destroyed. Consequently, the model requires the construction of detailed kinetic mechanisms. However, the construction of such models can not occur without sufficient data on key organic species. This provides part of the motivation for this work.

A further motivation for the present work stems from the desire to run the SCWO process autogenically, i.e. without external heating of the feed stream, thus reducing operating cost. To accomplish this the heating value of the waste stream must be large enough to preheat both the

waste stream and the oxidizer stream. In the MODAR process it was found that waste streams with heating values below 4.2 MJ/kg are candidates for addition of "auxiliary" or makeup fuel (Barner, *et al.*, 1992; Swallow, *et al.*, 1989). Since isopropanol has been identified as a candidate makeup fuel, further understanding of its oxidation characteristics in supercritical water is necessary.

Only a limited number of investigations concerning the oxidation of isopropanol in supercritical water appear in the literature. While none of these studies are adequate for detailed kinetic model development or validation, they are included here for completeness. Isopropanol is listed as "successfully treated by supercritical water oxidation" in a review by Tester *et. al* (1991). However, no species data or destruction efficiencies are presented. Acid–catalyzed dehydration reactions of *n*-propanol and isopropanol in supercritical water have been studied extensively by Antal and coworkers (Narayan and Antal, 1988; Narayan and Antal, 1990; Ramayya, *et al.*, 1987). Catalytic oxidation of isopropanol, at low temperatures (125–160 °C) and low pressures (2.32–6.55 bar), has been investigated by Akse and Jolly (1991). In that work acetone was identified as a key intermediate in the oxidation of isopropanol. In addition, it was found that acetone is harder than isopropanol to oxidize, a conclusion that will be examined in this paper. The catalytic oxidation of isopropanol was also reported by Krajnc and Levec (1994). Finally, two works appear regarding the atmospheric–pressure, gas–phase, oxidation of isopropanol. The first describes the enhanced oxidation rate of isopropanol in oxygen with the addition of H_2O_2 (Martinez, *et al.*, 1993). The second discusses the atmospheric–pressure oxidation of isopropanol to acetone on a copper catalyst (Buchin, *et al.*, 1989).

The experimental methods employed in the present work offer some distinct advantages over those used in past SCWO studies. By employing *in–situ* Raman spectroscopy it is possible to measure the absolute concentration of reactants, intermediates, and products simultaneously. In addition, because the optical access is conveniently translated along the length of the reactor, the entire reaction history, including production and destruction of key intermediates, is easily obtained. In addition, *in–situ* measurement eliminates possible errors associated with more

Species concentrations are calculated by integrating the area under the appropriate Raman peak and applying the necessary calibration factor. Calibration of the optical system is discussed below and in Rice, *et al.* (1995). The Raman signal was collected by taking the time averaged response for a 160 s exposure. Integration of the collected Raman signal over wavelength is a straight forward process when a single peak is present (see Figure 1a). However, when two peaks are present (Figure 1b) an approximation must be made to perform the integration. In this case the area of a peak is determined by integrating from its tail to the minimum point of the summed, overlap region (Figure 1b). This provides a reasonable approximation to the actual area since the peak overlap is not large. In addition, it is assumed that the area added to the original peak by the adjacent peak is approximately equal to the area removed from the original peak. To test this hypothesis, the error associated with the previous assumption was calculated. Each peak was assumed to be Gaussian, which is reasonable as evidenced by the fit in Figure 1a. Then the sum of the two Gaussian curves was fit to the observed data, using both prexponentials, offsets, and a common width as adjustable parameters. Each peak area was determined individually by integrating its Gaussian fit and was then compared to the area determined from the summed curve using the integration method noted above, i.e. integrating from the tail of a peak to the minimum point of the overlap region. For a worst case scenario, i.e., when the peak amplitudes have maximum difference, the approximation method produces an error of less than 7%. The uncertainty in determining the concentration by integration of a single peak, based solely of a statistical analysis of the noise, is less than ±2.5% (Rice, *et al.*, 1995).

System calibration was performed over the entire temperature range, 400 to 480 °C, by pumping a known concentration of isopropanol through the flow reactor optical module without oxidizer present. The resulting Raman signal was ratioed to the signal from the water O–H stretching resonance at 3628 cm^{-1} and a calibration curve was constructed. In this analysis, it is assumed that the concentration of isopropanol in the probe volume is known, i.e., for the temperature range employed the isopropanol does not pyrolize or oxidize due to trace concentrations of O_2 present in the water stream.

To test this assumption, pyrolysis experiments were performed over the entire experimental temperature range by introducing fuel in the absence of oxidizer. Then two Raman fuel concentration measurements were made, one at the minimum fuel flow rate (maximum fuel residence time in the heater subsystem) and the second at the maximum fuel flow rate (minimum fuel residence time in the heater subsystem). This change in flow rate corresponds to a factor of three change in residence time. If the integrated Raman signal, measured under these two conditions, does not change, we may conclude that no pyrolysis has occurred. Results indicate that below 450 °C no pyrolysis occurs for the residence times examined in this work. For temperatures above 450 °C, however, some pyrolysis does occur, but consumes less than 10% of the original fuel. This will slightly skew our calibration curve for the higher temperature, longer residence–time data (i.e., T > 450 °C and oxidation residence times > ~1 sec) and will cause a small overprediction in concentration for the data within this range. However, as will be shown below, under oxidation conditions with residence times > ~1 s and temperatures > 450 °C virtually all of the isopropanol has been consumed, therefore, small errors in the calibration curve are inconsequential as the concentration has already gone to zero.

At this time, due to pump–seal incompatibilities, the acetone Raman signal has not been individually calibrated. Based on results presented in Griffiths (1974), the differential cross section of acetone is assumed to be a factor 1.16 greater than that of isopropanol. Therefore, acetone concentrations are calculated by applying this scaling factor to the isopropanol calibration.

Experimental Procedure

Experiments were conducted under conditions of constant temperature, pressure, and initial mole fractions of fuel and oxidant, i.e., constant equivalence ratio[1]. The initial conditions for each experiment are listed in Table 1. Species concentration data were obtained by measuring the isopropanol and acetone concentrations at various residence times using Raman spectroscopy. The residence time was varied by adjusting the input flow rates of fuel and oxidant streams

[1]Equivalence ratio is defined as $\dfrac{(\text{moles isopropanol} / \text{moles } O_2)}{(\text{moles isopropanol} / \text{moles } O_2)_{\text{stoichiometric}}}$.

accordingly, while maintaining a constant equivalence ratio. All current results were generated with the optical module installed at a single point in the flow reactor facility. A total of nine experiments, numbered runs 1 through 9 in Table 1, were conducted at a nominally constant pressure of 24.4 MPa and temperatures ranging from 400–480 °C.

RESULTS AND DISCUSSION

One of the main objectives of this work is to obtain data on the supercritical water oxidation of isopropanol that are suitable for kinetic model development and validation. Presented in Table 2 are tabular results of the normalized concentration and residence–time data for isopropanol and acetone, the principal intermediate formed and subsequently destroyed during the oxidation. Normalized concentrations are defined as the measured species concentration, i.e., isopropanol, [ipa], or acetone, [ace], divided by the initial isopropanol concentration, $[ipa]_o$.

In Figure 2 the results for runs 2, 4, 6, and 8 are plotted. It is apparent from Figure 2, as expected, that the isopropanol disappearance rate increases with increasing temperature. This, in turn, directly impacts the production rate of acetone, which also increases with increasing temperature.

Despite the current lack of a detailed kinetic model to more thoroughly explore these data, it is possible to gain considerable insight through global kinetic analysis. Such models represent a consolidation of more complex reaction schemes and permit an initial indication of species reactivity. For the current analysis, first–order kinetics is assumed for the destruction of both isopropanol and acetone. This type of analysis has been used in the reduction of SCWO data in the past and has been found to provide a reasonable representation of the experimental data (Tester, *et al.*, 1991).

When the destruction of isopropanol is assumed to be first–order with respect to fuel and zeroth–order with respect to oxygen, the following equation is obtained

$$\frac{d[ipa]}{dt} = -k_{eff,ipa}[ipa] \qquad (1)$$

where $k_{eff,\,ipa}$ is the effective first–order rate constant. For each experiment in which sufficient data was acquired (i.e., at least two points, runs 1 through 7), a linear, least squares fit was performed on the natural logarithm of normalized isopropanol concentration versus residence–time data. The slope of this fit gives $k_{eff,\,ipa}$ and the intercept at a normalized isopropanol concentration of unity corresponds to the apparent induction time, t_{ind}. If it is assumed that $k_{eff,\,ipa}$ has an Arrhenius behavior, then both the preexponential, A, and the activation energy, E_a, can be calculated by performing a linear fit of $\ln(k_{eff,\,ipa})$ versus 1/T, see Figure 3. The analysis gives $E_{a,\,ipa} = 301.1$ kJ·mol^{-1} and $A_{ipa} = 3.255 \times 10^{22}$ s^{-1}.

The experimental results for isopropanol indicate that there is a temperature dependent induction time, t_{ind}, i.e., a time after entry of the reactant mixture into the flow reactor during which, little to no reaction occurs. Therefore, to compare the calculated first–order kinetic results to the experimental data it is necessary to calculate or estimate t_{ind} for each of the data sets. The induction time was determined for runs 3–7 by extrapolation to a normalized isopropanol concentration of unity, as previously discussed. It is apparent that t_{ind}, for runs 3–7, is roughly linearly dependent on temperature, see Figure 4. For runs 1 and 2 the change in the concentration of isopropanol is sufficiently small that noise in the measurement results in induction times that are unreasonable. For runs 8 and 9 there is not sufficient data to extrapolate the concentration measurements. Therefore, the linear fit was used to approximate the induction times for runs 1, 2, 8, and 9.

To compare the first–order model to the experimental data, Equation 1 must be integrated from $[ipa]_o$ to [ipa] for isopropanol concentration and from t_{ind} to t for residence time to obtain

$$\frac{[ipa]}{[ipa]_o} = \exp\left(-k_{eff,ipa} \cdot \left(t - t_{ind}\right)\right) \quad \text{for } t \geq t_{ind}. \tag{2}$$

For residence times less than the induction time the normalized concentration is set to unity. The model and experimental results are plotted in Figure 5. It is apparent that first–order kinetics reproduce the experimental data reasonably well.

Since acetone is simultaneously produced and destroyed during the isopropanol oxidation process, examining its destruction rate is more difficult. If, however, it is possible to extract concentration data where the production rate is sufficiently small, then the destruction rate can be effectively determined. For the current analysis it is assumed that normalized isopropanol concentrations below 10% of the original value are acceptably small. In Figure 6, the normalized acetone concentration is plotted versus residence time for conditions meeting the above criterion, i.e., $[ipa]/[ipa]_o < 0.1$. This plot indicates that, as for isopropanol, the disappearance rate of acetone increases with increasing temperature.

Using this bounded acetone data set, i.e., acetone concentrations when $[ipa]/[ipa]_o < 0.1$, it is possible to obtain an effective first–order rate constant for the destruction of acetone by following a method similar to that used for determining the effective rate for isopropanol. If it is assumed that the destruction rate of acetone is first–order with respect to acetone and zeroth–order with respect to oxygen, then an effective first–order rate constant, $k_{eff,\,ace}$, can be determined for the data shown in Figure 6. If it is assumed that $k_{eff,\,ace}$ has Arrhenius dependence, then both the preexponential factor and the activation energy can be calculated by performing a linear least squares fit of $\ln(k_{eff,\,ace})$ versus 1/T. This analysis gives $E_{a,\,ace} = 85.12$ kJ·mol^{-1} and $A_{ace} = 2.233 \times 10^6$ s^{-1}. While this analysis is reasonable, it only allows the use of a small fraction of the experimental data. With an additional assumption regarding the production of acetone, a more rigorous analysis can be performed allowing all of the experimental data to be used in the fit of $k_{eff,\,ace}$.

If it is assumed that all of the isopropanol that is destroyed proceeds through the acetone channel, then the destruction rate of isopropanol is equal to the production rate of acetone. If we again assume that the destruction of acetone is first–order with respect to acetone and zeroth–order with respect to oxygen, it is possible to write the following equation for the total rate of change of the acetone concentration

$$\frac{d[ace]}{dt} = k_{eff,ipa}[ipa] - k_{eff,ace}[ace]. \qquad (3)$$

Equation 3 can be integrated analytically (given the boundary condition [ace] at $t = t_{tind}$ is equal to 0) to give the following equation for the evolution of acetone

$$\frac{[ace]}{[iso]_o} = \frac{k_{eff,ipa}}{k_{eff,ace} - k_{eff,ipa}} \left\{ \exp\left[-k_{eff,ipa} \cdot (t - t_{ind})\right] - \exp\left[-k_{eff,ace} \cdot (t - t_{ind})\right] \right\} \quad \text{for } t \geq t_{ind}. \quad (4)$$

The only unknown in this equation is $k_{eff,\ ace}$, which, if Arrhenius behavior is assumed, is dependent on A_{ace} and $E_{a,\ ace}$. Using our experimental data, these parameters were determined by minimizing the square of the error between the predicted and the observed value of the normalized acetone concentration, giving $E_{a,\ ace} = 137.7$ kJ·mol^{-1} and $A_{ace} = 1.948 \times 10^{10}$ s^{-1}. In this analysis we have assumed that during the induction time little to no reaction of isopropanol occurs, therefore, we have also assumed that no acetone is formed during the induction time, i.e., for residence times less than the induction time the concentration of acetone is zero.

Using these parameters for $E_{a,\ ace}$ and A_{ace} and the previously determined values of t_{ind} and $k_{eff,\ ipa}$, the normalized concentration of acetone can be calculated with equation 4. These results are plotted along with the experimental data in Figure 7. It is again evident that even with this rudimentary model for the oxidation of isopropanol and acetone, first–order kinetics (with an induction time) does a reasonable job of approximating the production and destruction of acetone in this system.

Finally, it is interesting to compare the two calculated first–order rate constants for acetone oxidation and to compare these constants to that determined for isopropanol. In Figure 8 the three rate constants are shown over the temperature range of the current work. In the figure, $k_{eff,\ ace(T\ high)}$ represents the rate constant calculated based on the first method discussed, i.e., using the constrained ($[ipa]/[ipa]_o < 0.1$), high temperature acetone results. This rate constant compares quite favorably to the rate constant determined using the full acetone data set, represented by $k_{eff,\ ace}$. While the second method requires an additional assumption, it allows a more thorough fit, using all of the experimental acetone concentration data. Both rate constants intersect the isopropanol rate constant at ~425 °C. Below 425 °C $k_{eff.\ ace(T\ high)} > k_{eff,\ ace}$; however, their maximum deviation is less than a factor of 1.4. Above 425 °C $k_{eff,\ ace} > k_{eff.\ ace(T\ high)}$; the

maximum deviation is again small, less than a factor of 2. The current results indicate that for temperatures above 425 °C and pressures of approximately 24.4 MPa that acetone is more difficult to oxidize than isopropanol, while below 425 °C the opposite is true. Preliminary results from our lab for temperatures extending into the subcritical temperature region (350–400 °C) support the observation that the acetone destruction rate is faster than that of isopropanol for lower temperatures.

CONCLUSIONS

The oxidation of isopropanol in supercritical water has been examined using Raman spectroscopy. The use of Raman spectroscopy as an *in-situ* diagnostic eliminates potential perturbations of the reacting system during sampling and allows reactants, intermediates, and products of the oxidation process to be simultaneously measured. It was found that acetone is a key intermediate produced in the oxidation process. Extensive data, in the form of measured concentrations of isopropanol and acetone as a function of residence time, are presented and analyzed.

Assuming first–order kinetics for the destruction of isopropanol an effective first–order rate constant, $k_{eff,\,ipa}$, is determined, viz.,

$$k_{eff,ipa} = 3.255 \times 10^{22} (s^{-1}) \exp\left(\frac{-301.1 (kJ \cdot mol^{-1})}{RT} \right).$$

By additionally assuming that the production rate of acetone is equal to the destruction rate of isopropanol and that the destruction of acetone follows first–order kinetics, an effective first–order rate constant for acetone, $k_{eff,\,ace}$, is determined, viz.,

$$k_{eff,ace} = 1.948 \times 10^{10} (s^{-1}) \exp\left(\frac{-137.7 (kJ \cdot mol^{-1})}{RT} \right).$$

Based on these results it is apparent that the destruction of isopropanol occurs more rapidly than the destruction of acetone over most of the temperature range examined in this work.

Current experiments are investigating the supercritical water oxidation of normal alcohols, e.g., *n*-propanol and ethanol. The goals are to examine the differences between the oxidation channels and the formation of intermediates between the primary and secondary simple alcohols. This data will be useful both for detailed kinetic model development and validation and for the insights that data will provide regarding the use of these fuels as auxiliary make–up fuels for the SCWO process.

ACKNOWLEDGMENTS

This work was supported by the DoD/DOE/EPA Strategic Environmental Research and Development Program. We thank Å. C. Rydén (Lund University) for technical assistance.

LITERATURE CITED

Ahluwalia, K. S.; Young, M. F.; Haroldsen, B. L.; Mills, B. E.; Stoddard, M. C.; Robinson, C. D. Testing and Application of a Transpiring Wall Platelet Reactor for Supercritical Water Oxidation of Hazardous Waste. First International Workshop on Supercritical Water Oxidation, Jacksonville, Florida, 1995, Session VI: Innovative Reactor Design to Mitigate Corrosion Effects.

Akse, J. R.; Jolly, C. D. Catalytic Oxidation for Treatment of ECLSS & PMMS Waste Streams. *SAE Trans J. Aero-Section 1* **1991**, *100,* 1716-1725.

Barner, H. E.; Huang, C. Y.; Johnson, T.; Martch, M. A.; Killilea, W. R. Supercritical Water Oxidation: An Emerging Technology. *J. Hazard. Mater.* **1992**, *31,* 1-17.

Brennecke, J. F. Chapter 16, Spectroscopic Investigations of Reactions in Supercritical Fluids. In *Supercritical Fluid Engineering Science Fundamentals and Applications*; Kiran, E. and Brennecke, J. F., Eds.; American Chemical Society: Washington, DC, 1991; Vol. 514, pp 201-219.

Buchin, V. A.; Lyubimov, G. A.; Rumyantsev, P. G.; Trifonov, V. D. Oxidation of Isopropanol to Acetone on a Copper Catalyst in a Flow-Type Chemical Reactor Under Stable and Unstable Operation Regimens. Academy of Sciences of the USSR, Proceedings, Chemical Technology Section, 1989, 12-15.

Gloyna, E. F.; Li, L.; McBrayer, R. N. Engineering Aspects of Supercritical Water Oxidation. *Water Sci. Technol.* **1994**, *30,* (9), 1-10.

Grasselli, J. G.; Bulkin, B. J. *Analytical Raman Spectroscopy*; John Wiley & Sons, Inc.: New York, 1991; Vol. 114.

Griffiths, J. E. Raman Scattering Cross Sections in Strongly Interacting Liquid Systems: CH_3OH, C_2H_5OH, i-C_3H_7OH, $(CH_3)_2CO$, H_2O, and D_2O. *J. Chem. Phys.* **1974**, *60,* (6), 2556-2557.

Hanush, R. G.; Rice, S. F.; Hunter, T. B. "Operation and Performance of the Super Critical Water Oxidation Flow Reactor (SCWOFR)," Sandia National Laboratories, Technical Report No. *submitted*, 1995.

Kemna, A. H.; Kuharich, E. MODEC's SCWO Pilot Plant and its Monitoring and Control System. First International Workshop on Supercritical Water Oxidation, Jacksonville, Florida, 1995, Session V: SCWO Systems Design, Monitoring, Instrumentation.

Krajnc, M.; Levec, J. Catalytic Oxidation of Toxic Organics in Supercritical Water. *Appl. Catal. B: Environmental* **1994**, *3,* L101-L107.

Martinez, A.; Geiger, C.; Hewett, M.; Clausen, C. A.; Cooper, C. D. Using Hydrogen Peroxide or Ozone to Enhance the Incineration of Volatile Organic Vapors. *Waste Manage.* **1993**, *13,* 261-270.

McBrayer, R. N. Design and Operation of the First Commercial Supercritical Water Oxidation Facility. First International Workshop on Supercritical Water Oxidation, Jacksonville, Florida, 1995, Session IV: SCWO Technology Development Demonstrations.

Modell, M. "Processing Methods for the Oxidation of Organics in Supercritical Water."; U.S. Patent 4,543,190, September 24, 1985.

Modell, M. Section 8.11, Supercritical-Water Oxidation. In *Standard Handbook of Hazardous Waste Treatment and Disposal*; Freeman, H. M., Ed. McGraw-Hill: New York, 1989; pp 8.153-8.167.

Narayan, R.; Antal, M. J., Jr. Kinetic Elucidation of the Acid-Catalyzed Mechanism of 1-Propanol Dehydration in Supercritical Water, Chapter 15. In *Supercritical Fluid Science and Technology*; Johnston, K. P. and Penninger, J. M. L., Eds.; American Chemical Society: Washington, DC, 1988; Vol. 406, pp 226-241.

Narayan, R.; Antal, M. J., Jr. Influence of Pressure on the Acid-Catalyzed Rate Constant for 1-Propanol Dehydration in Supercritical Water. *J. Am. Chem. Soc.* **1990**, *112,* 1927-1931.

Ramayya, S.; Brittain, A.; DeAlmeida, C.; Mok, W.; Antal, M. J., Jr. Acid-catalyzed Dehydration of Alcohols in Supercritical Water. *Fuel* **1987**, *66,* 1365-1372.

Rice, S. F.; Hunter, T. B.; Rydén, Å. C.; Hanush, R. G. Raman Spectroscopic Measurement of Oxidation in Supercritical Water. I. Conversion of Methanol to Formaldehyde. *submitted Ind. Eng. Chem. Res.* **1995**.

Sadtler *The Sadtler Standard Raman Spectra*; Sadtler Research Laboratories, subsidiary of Block Engineering: Philadelphia, PA, 1973.

Shaw, R. W.; Brill, T. B.; Clifford, A. A.; Eckert, C. A.; Franck, E. U. Supercritical Water. *Chem. & Eng. News* **1991**, *69,* 26-39.

Steeper, R. R.; Rice, S. F. Supercritical Water Oxidation of Hazardous Wastes. AIAA, 31st Aerospace Sciences Meeting & Exhibit, Reno, NV, 1993, 1-9.

Swallow, K. C.; Killilea, W. R.; Malinowski, K. C.; Staszak, C. N. The MODAR Process for the Destruction of Hazardous Organic Wastes-Field Test of a Pilot-Scale Unit. *Waste Manage.* **1989**, *9,* 19-26.

Tester, J. W.; Holgate, H. R.; Armellini, F. J.; Webley, P. A.; Killilea, W. R.; Hong, G. T.; Barner, H. E. Chapter 3, Supercritical Water Oxidation Technology Process Development and Fundamental Research. In *Emerging Technologies in Hazardous Waste Management III*; Tedder, D. W. and Pohland, F. G., Eds.; American Chemical Society: Washington, DC, 1991; Vol. 518, pp 35-76.

Thomason, T. B.; Hong, G. T.; Swallow, K. C.; Killilea, W. R. *Innovative Hazardous Waste Treatment Technology Series*; Freeman, H. M., Ed. Technomic Publishing Co.: Lancaster, PA, 1990; Vol. 1: Thermal Processes, pp 31-42.

Thomason, T. B.; Modell, M. Supercritical Water Destruction of Aqueous Wastes. *Hazard. Waste* **1984**, *1,* 453.

Table 1 Experimental Conditions [a]

Run	Temp (°C)	Pressure (bar)	Initial Mole Fraction O_2	Initial Mole Fraction Isopropanol
1	400 ± 0	244 ± 1	0.0169 ± 0.0003	0.00328 ± 0.00007
2	409 ± 3	245 ± 2	0.0169 ± 0.0002	0.00329 ± 0.00005
3	420 ± 2	244 ± 7	0.0169 ± 0.0002	0.00329 ± 0.00004
4	430 ± 1	244 ± 1	0.0168 ± 0.0001	0.00330 ± 0.00003
5	440 ± 0	245 ± 3	0.0169 ± 0.0002	0.00329 ± 0.00004
6	450 ± 2	244 ± 1	0.0168 ± 0.0003	0.00331 ± 0.00007
7	460 ± 2	245 ± 2	0.0169 ± 0.0002	0.00329 ± 0.00003
8	470 ± 1	245 ± 2	0.0169 ± 0.0001	0.00329 ± 0.00002
9	480 ± 2	244 ± 5	0.0168 ± 0.0002	0.00329 ± 0.00003

[a] Conditions listed are the nominal initial conditions for each experiment. The listed uncertainties are ± 2 × (standard deviation) of the experimental data for each run.

Table 2 Experimental Measurements of Normalized Isopropanol and Acetone Concentrations [a]

Run 1, T = 400 °C			Run 2, T = 409 °C			Run 3, T = 420 °C		
t (s)	$\frac{[ipa]}{[ipa]_o}$	$\frac{[ace]}{[ipa]_o}$	t (s)	$\frac{[ipa]}{[ipa]_o}$	$\frac{[ace]}{[ipa]_o}$	t (s)	$\frac{[ipa]}{[ipa]_o}$	$\frac{[ace]}{[ipa]_o}$
0.79	0.98	0.02	0.72	0.95	0.03	0.63	0.92	0.06
1.07	0.87	0.04	0.97	0.92	0.03	0.92	0.93	0.12
1.41	0.82	0.08	1.27	0.88	0.10	1.20	0.79	0.18
1.82	0.76	0.08	1.60	0.87	0.13	1.43	0.72	0.22
2.02	0.82	0.09	1.90	0.80	0.11	1.68	0.48	0.32
2.41	0.77	0.11	2.23	0.66	0.21	2.00	0.32	0.39
Run 4, T = 430 °C			**Run 5, T = 440 °C**			**Run 6, T = 450 °C**		
t (s)	$\frac{[ipa]}{[ipa]_o}$	$\frac{[ace]}{[ipa]_o}$	t (s)	$\frac{[ipa]}{[ipa]_o}$	$\frac{[ace]}{[ipa]_o}$	t (s)	$\frac{[ipa]}{[ipa]_o}$	$\frac{[ace]}{[ipa]_o}$
0.58	0.84	0.03	0.58	0.84	0.24	0.56	0.71	0.19
0.82	0.82	0.13	0.77	0.72	0.27	0.73	0.44	0.33
1.09	0.51	0.22	1.03	0.30	0.44	0.97	0.09	0.40
1.36	0.26	0.31	1.26	0.07	0.47	1.21	0.00	0.33
1.55	0.07	0.40	1.47	0.01	0.42	1.34	0.00	0.27
1.85	0.00	0.40	1.70	0.02	0.34	1.62	0.01	0.15
Run 7, T = 460 °C			**Run 8, T = 470 °C**			**Run 9, T = 480 °C**		
t (s)	$\frac{[ipa]}{[ipa]_o}$	$\frac{[ace]}{[ipa]_o}$	t (s)	$\frac{[ipa]}{[ipa]_o}$	$\frac{[ace]}{[ipa]_o}$	t (s)	$\frac{[ipa]}{[ipa]_o}$	$\frac{[ace]}{[ipa]_o}$
0.52	0.56	0.41	0.49	0.23	0.42	0.48	0.06	0.28
0.71	0.11	0.40	0.68	0.02	0.43	0.64	0.00	0.19
0.94	0.04	0.37	0.90	0.00	0.25	0.87	0.00	0.08
1.17	0.00	0.22	1.11	0.02	0.12	1.11	0.02	0.04
1.34	0.00	0.16	1.29	0.02	0.12	1.27	0.00	0.01
1.55	0.02	0.10	1.53	0.02	0.07	1.48	0.02	0.03

[a] t (s) = residence time (s), $\frac{[ipa]}{[ipa]_o} = \frac{\text{isopropanol concentration}}{\text{isopropanol concentration}_{initial}}$, $\frac{[ace]}{[ipa]_o} = \frac{\text{acetone concentration}}{\text{isopropanol concentration}_{initial}}$.

FIGURE CAPTIONS

Figure 1 Raman spectra for run 3 (420°C). (a) At a short residence–time, 0.63 s, very little isopropanol has oxidized and no acetone has been produced, therefore, only an isopropanol peak is visible, a Gaussian fit is also shown. (b) At a longer residence–time, 2.0 s, both the isopropanol and acetone peaks are visible.

Figure 2 Measured normalized species concentration profiles plotted versus residence–time for (a) isopropanol and (b) acetone, runs 2 (409°C) ○, 4 (430°C) □, 6 (450°C) △, and 8 (470°C) ▽.

Figure 3 Effective first order rate constants for isopropanol destruction (runs 1-7) plotted versus 1000/T (the line is calculated from a linear least squares fit of the data).

Figure 4 Measured induction times for isopropanol destruction (runs 3-7) plotted versus temperature (the line is calculated from a linear least squares fit of the data).

Figure 5 Comparison of calculated first order reaction kinetics (lines) to isopropanol experimental data (open symbols) for runs 2 (409°C) ○ ———, 4 (430°C) □ — — -, 6 (450°C) △ - - - - -, and 8 (470°C) ▽ — - -.

Figure 6 Measured acetone concentration plotted versus residence–time for conditions when the normalized isopropanol concentration is less than 0.1, runs 6 (450°C) ○, 7 (460°C) □, 8 (470°C) △, and 9 (480°C) ▽.

Figure 7 Comparison of calculated first order reaction kinetics (lines), to acetone experimental data (open symbols) for runs 2 (409°C) ○ ———, 4 (430°C) □ — — -, 6 (450°C) △ - - - - -, and 8 (470°C) ▽ — - -.

Figure 8 Comparison of the calculated effective first order rate constants for the oxidation of isopropanol, $k_{eff,\ ipa}$ ———, and acetone (using two different fitting methods) $k_{eff,\ ace}$ - - - - - and $k_{eff,\ ace(T\ high)}$ — — -.

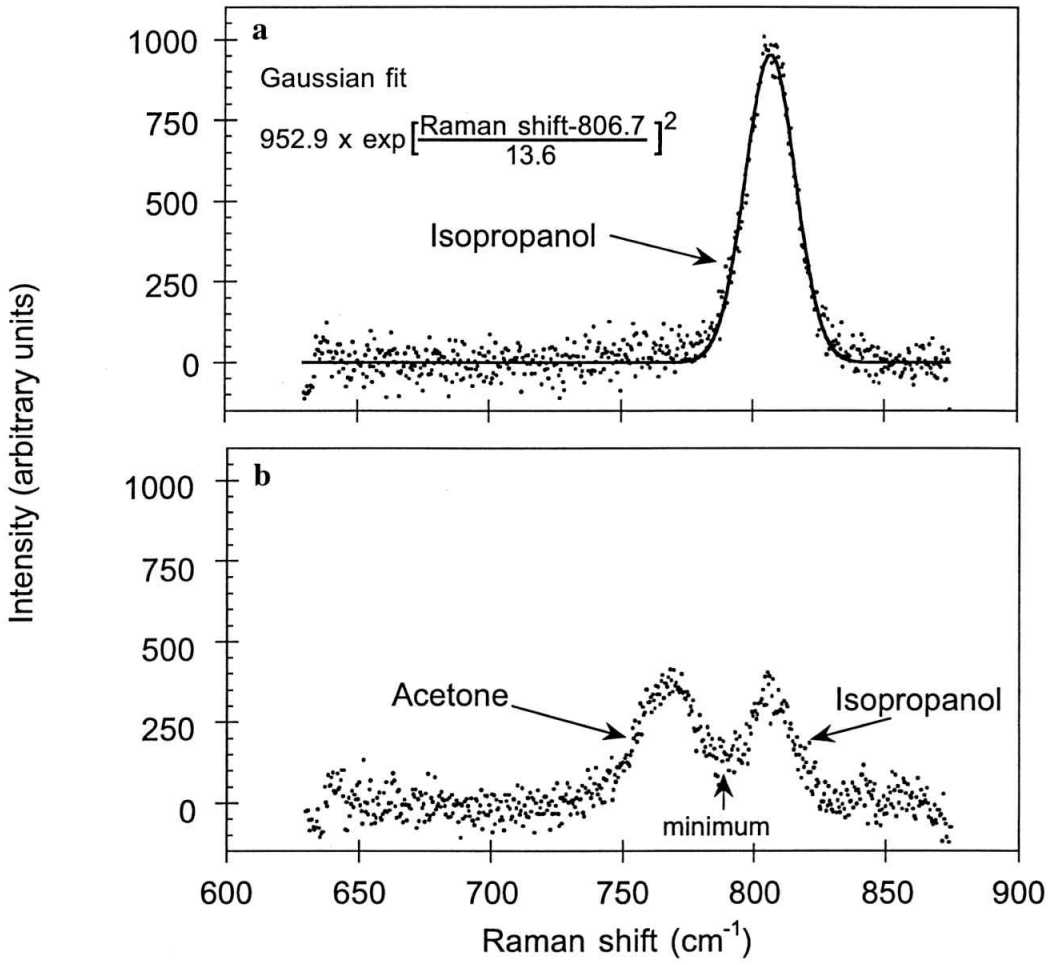

Figure 1 Raman spectra for run 3 (420°C). (a) At a short residence–time, 0.63 s, very little isopropanol has oxidized and no acetone has been produced, therefore, only an isopropanol peak is visible, a Gaussian fit is also shown. (b) At a longer residence–time, 2.0 s, both the isopropanol and acetone peaks are visible.

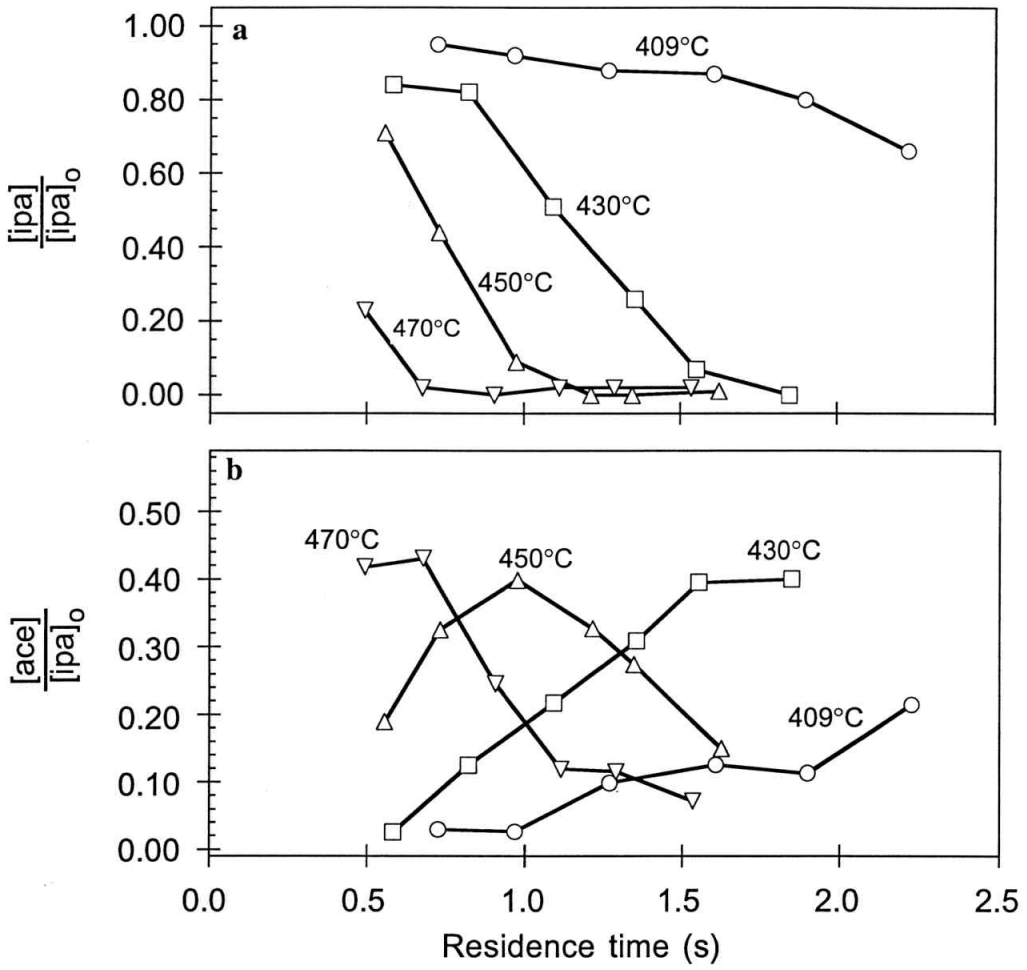

Figure 2 Measured normalized species concentration profiles plotted versus residence–time for (a) isopropanol and (b) acetone, runs 2 (409°C) ○, 4 (430°C) □, 6 (450°C) △, and 8 (470°C) ▽.

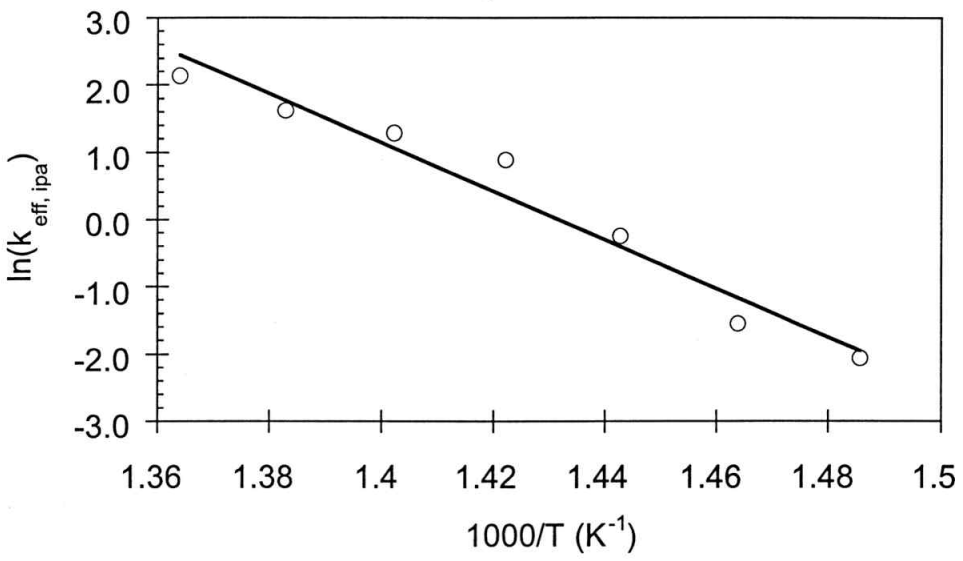

Figure 3 Effective first order rate constants for isopropanol destruction (runs 1-7) plotted versus 1000/T (the line is calculated from a linear least squares fit of the data).

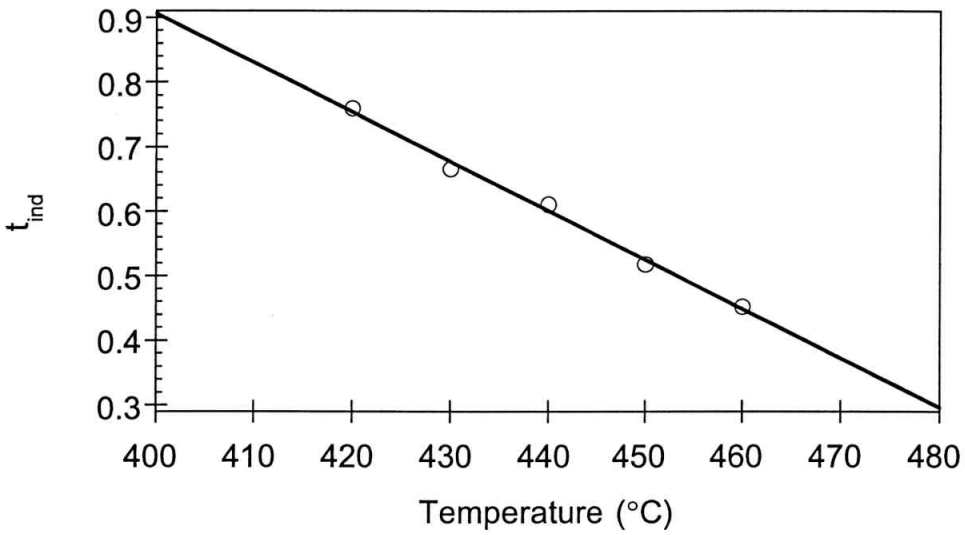

Figure 4 Measured induction times for isopropanol destruction (runs 3-7) plotted versus temperature (the line is calculated from a linear least squares fit of the data).

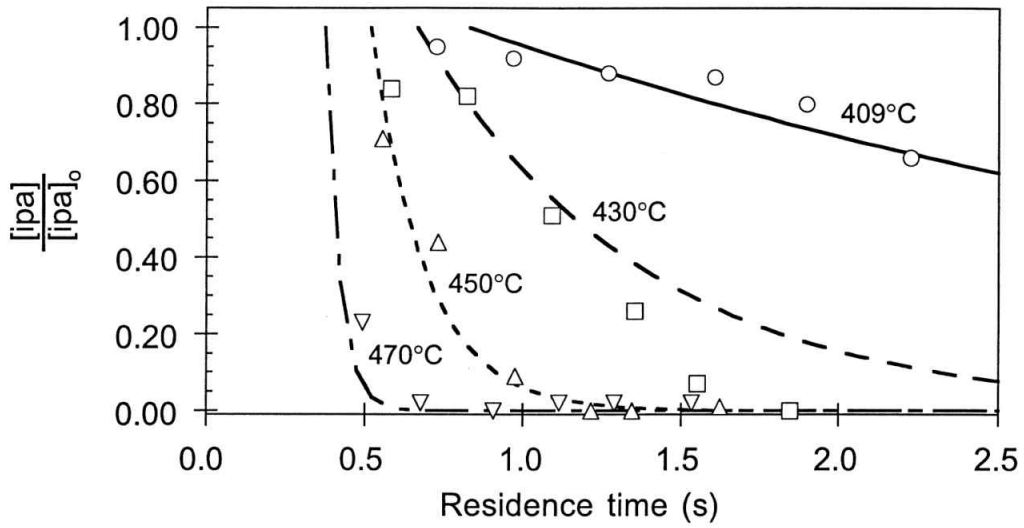

Figure 5 Comparison of calculated first order reaction kinetics (lines) to isopropanol experimental data (open symbols) for runs 2 (409°C) ○ ——— , 4 (430°C) □ — — - , 6 (450°C) △ - - - - - , and 8 (470°C) ▽ — - - .

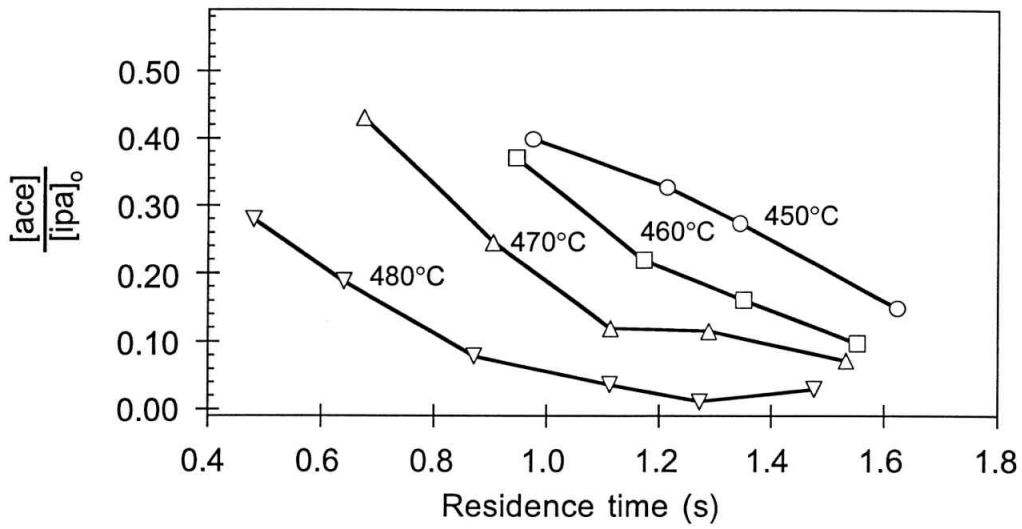

Figure 6 Measured acetone concentration plotted versus residence–time for conditions when the normalized isopropanol concentration is less than 0.1, runs 6 (450°C) ○, 7 (460°C) □, 8 (470°C) △, and 9 (480°C) ▽.

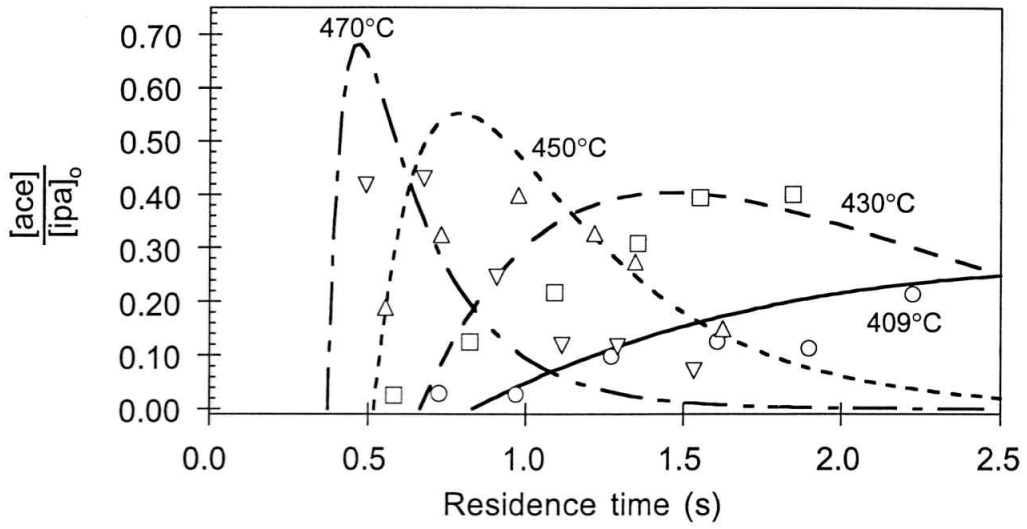

Figure 7 Comparison of calculated first order reaction kinetics (lines), to acetone experimental data (open symbols) for runs 2 (409°C) ○ ——— , 4 (430°C) □ — — - , 6 (450°C) △ - - - - - , and 8 (470°C) ▽ — - - .

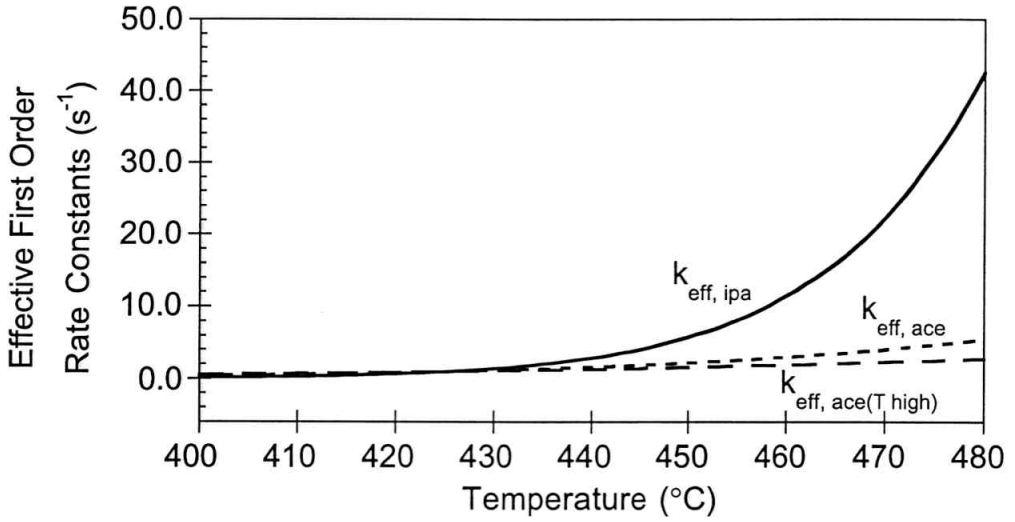

Figure 8 Comparison of the calculated effective first order rate constants for the oxidation of isopropanol, $k_{eff, ipa}$ ——— , and acetone (using two different fitting methods) $k_{eff, ace}$ - - - - - and $k_{eff, ace(T high)}$ — — -.